NAVAL POSTGRADUATE SCHOOL

MONTEREY, CALIFORNIA

THESIS

STRAIN-BASED DISPLACEMENT ESTIMATION FOR PRECISION SPACECRAFT STRUCTURES

by

Craig S. Coleman

December 2005

Thesis Advisor: Brij N. Agrawal
Co-Advisor: Donald Walters

Approved for public release, distribution is unlimited

THIS PAGE INTENTIONALLY LEFT BLANK

REPORT DOCUMENTATION PAGE

Form Approved OMB No. 0704-0188

1. AGENCY USE ONLY *(Leave blank)*	2. REPORT DATE	3. REPORT TYPE AND DATES COVERED
	December 2005	Master's Thesis

4. TITLE AND SUBTITLE Title

Strain-Based Displacement Estimation For Precision Spacecraft Structures

5. FUNDING NUMBERS

6. AUTHOR (S) Coleman, Craig S.

7. PERFORMING ORGANIZATION NAME(S) AND ADDRESS(ES)
Naval Postgraduate School
Monterey, CA 93943-5000

8. PERFORMING ORGANIZATION REPORT NUMBER

9. SPONSORING / MONITORING AGENCY NAME(S) AND ADDRESS(ES)

10. SPONSORING/MONITORING AGENCY REPORT NUMBER

11. SUPPLEMENTARY NOTES The views expressed in this thesis are those of the author and do not reflect the official policy or position of the U.S. Department of Defense or the U.S. Government.

12a. DISTRIBUTION / AVAILABILITY STATEMENT
Approved for public release; distribution unlimited.

12b. DISTRIBUTION CODE

13. ABSTRACT ***(maximum 200 words)***

For precision spacecraft structures used for antennas and reflectors of telescopes, determination of in-orbit structural displacement and its control is very important. While this kind of measurement is relatively easy to carry out in a laboratory setting, it can be problematic in a real world environment. A procedure for the real-time determination of displacements at any point of a vibrating body can be utilized by measuring strain that is present. The procedure could employ measurement devices like Fiber Bragg Gratings, which are capable of very fine strain measurements. This thesis presents the finite element analysis of a truss similar to the NPS Space truss to observe the behavior of the strain relative to the displacement. A relationship between strain and displacement for the truss is derived.

14. SUBJECT TERMS	15. NUMBER OF PAGES
Strain, Modeshapes, Finite Element Model, Bragg gratings	49
	16. PRICE CODE

17. SECURITY CLASSIFICATION OF REPORT	18. SECURITY CLASSIFICATION OF THIS PAGE	19. SECURITY CLASSIFICATION OF ABSTRACT	20. LIMITATION OF ABSTRACT
Unclassified	Unclassified	Unclassified	UL

NSN 7540-01-280-5500

Standard Form 298 (Rev. 2-89)
Prescribed by ANSI Std. 239-18

THIS PAGE INTENTIONALLY LEFT BLANK

Approved for public release; distribution is unlimited

STRAIN-BASED DISPLACEMENT ESTIMATION FOR PRECISION SPACECRAFT STRUCTURES

Craig S. Coleman
Lieutenant Commander, United States Navy
B.S., Hampton University, 1992

Submitted in partial fulfillment of the
Requirements for the degree of

MASTER OF SCIENCE IN ASTRONAUTICAL ENGINEERING

From the

NAVAL POSTGRADUATE SCHOOL
December 2005

Author: Craig S. Coleman

Approved by: Brij N. Agrawal
Thesis Advisor

Donald Walters
Thesis Co-Advisor

Tony Healey
Chairman, Department of Mechanical and
Astronautical Engineering

THIS PAGE INTENTIONALLY LEFT BLANK

ABSTRACT

For precision spacecraft structures used for antennas and reflectors of telescopes, determination of in-orbit structural displacement and its control is very important. While this kind of measurement is relatively easy to carry out in a laboratory setting, it can be problematic in a real world environment. A procedure for the real-time determination of displacements at any point of a vibrating body can be utilized by measuring strain that is present. The procedure could employ measurement devices like Fiber Bragg Gratings, which are capable of very fine strain measurements. This thesis presents the finite element analysis of a truss similar to the NPS Space truss to observe the behavior of the strain relative to the displacement. A relationship between strain and displacement for the truss is derived. From this relationship and the strain measurements, deflection at successive nodes was computed and compared to a Nastran simulation of the truss displacements.

THIS PAGE INTENTIONALLY LEFT BLANK

TABLE OF CONTENTS

THIS PAGE INTENTIONALLY LEFT BLANK

LIST OF FIGURES

THIS PAGE INTENTIONALLY LEFT BLANK

LIST OF TABLES

THIS PAGE INTENTIONALLY LEFT BLANK

I. INTRODUCTION

There has been and continues to be extensive work done in determining a relationship to estimate structural displacement based on measuring its strain. Gaukroger and Hassal [Ref. 1] selected a suitable group of strain gage patterns and corresponding displacements for a non-rotating cantilever beam that could be used to approximate the displacements for a helicopter blade. The objective was to obtain good agreement between the measured and fitted strain gage patterns for the stationary blade by omitting or adding modes as necessary. Displacements for the rotating case were then obtained from the modal coordinates obtained from the strain modes and the measured displacement mode shapes of the stationary condition. Foss and Haugse [Ref. 2] developed a transformation from strain to displacement for a cantilever plate using displacement modal testing in conjunction with strain modal testing. The modal coordinates again were approximated using the measured strains, strain modes and least squares. Optimal number and placement of the sensors were obtained using generic algorithms. Davis et al. [Ref. 3] assumed that the strain measured at any point could be written as a linear combination of a set of polynomials. These polynomials formed the strain basis functions, which upon successive integrations and application of the boundary conditions yielded the displacements at any point. In a subsequent study, Kirby et al. [Ref. 4] approximated the strain distribution as a linear combination of sines and polynomials. The polynomial guarantees a nonzero strain at the root. Again, the coefficients on the basis functions were determined using least squares and the displacements

were determined from these coefficients, successive integrations of the basis functions and imposition of the boundary conditions. It was demonstrated that the optimal sensor placement depends largely on the basis functions selected.

An alternative to global basis functions is the use of local basis functions. For this technique, the beam is discretized into a number of elements. Baz et al. [Ref. 5] assumed the curvature varied linearly over the length of each element. The strain sensors were located on the interior of each element. This assumption was used by Gopinathan et al. [Ref. 6]. but with the strain sensors located at the boundaries of each element. A major deficiency of the assumption of linear curvature over each element is loss of accuracy of the estimation as the curvature over each segment departs from linearity. Therefore, it should not be expected to obtain good results for higher modes or more complex deformations with a limited number of sensors. Accordingly, Vurpillot et al. [Ref. 7] examined the use quadratic curvatures over the length of the element. Andersson and Crawley [Ref.8] examined integration of the curvature using both the trapezoidal and Simpson rules. They also considered modeshape fitting as outlined in the previous paragraph, as well as the use of shaped strain sensors to obtain global shape estimates.

In this thesis I have examined the utility of measuring strain to determine modeshapes, in order to control vibration in large, flexible, space structures. I simulated the strain and displacement on a Precision Space Truss as the model for the structures of interest.

II. PRECISION SPACE TRUSS

A. DETAILED TRUSS DESCRIPTION

1. Elements

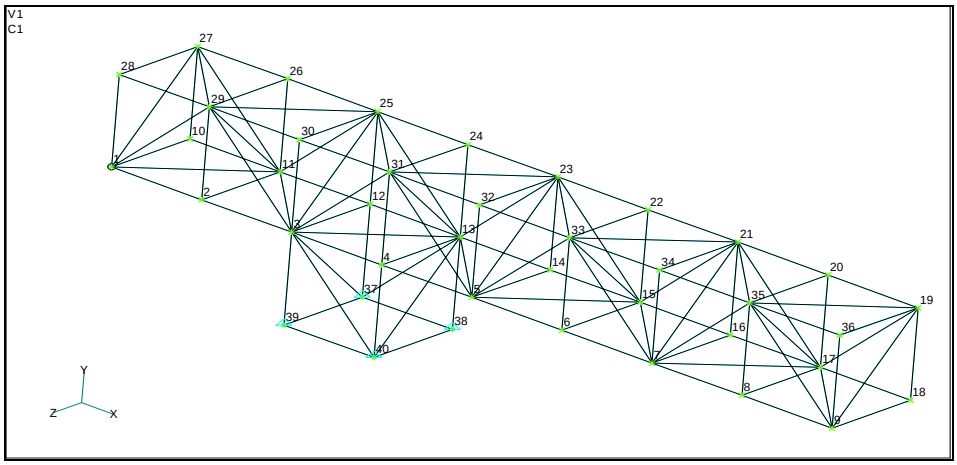

Figure 1. Precision Space Truss (with numbered nodes)

These eight cubic bays are a combination of battens/longerons and diagonals (see Figure 1). Longerons run down the length of the structure, battens compose the vertical elements, and diagonals run diagonally from one line of longerons to an adjacent line. Collectively, all of the aforementioned elements will be referred to as struts. Each strut is made of a composite material, and is composed of several parts: the tube, outer sleeve, bolt, standoff, and nut (see Figure 2). Additionally, the tube is fastened to the outer sleeve with epoxy and then a pin is driven through the sleeve and tube. Each strut begins and terminates in an Aluminum node ball.

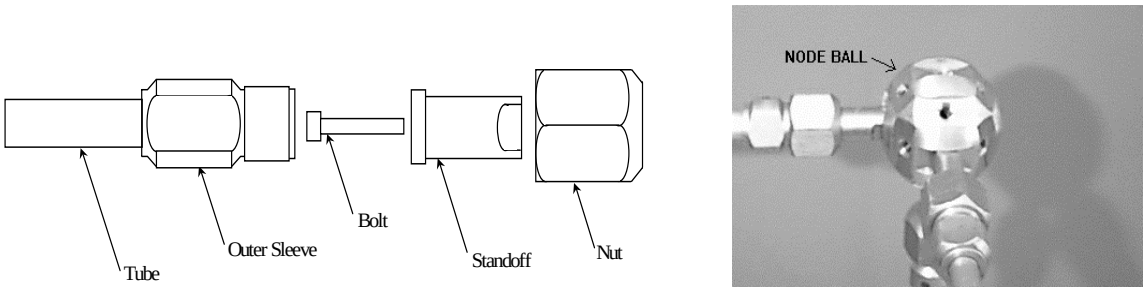

Figure 2. Strut Terminating End and Node Ball

The struts can be modeled as rod elements. Rods can be defined as elements whose geometry is such that the longest dimension of the bar is straight and the greatest dimension of the cross section is small compared to the length. A rod is an axial member with an internal axial force only, known as a two-force member. Figure 3 is a basic schematic for a rod element.

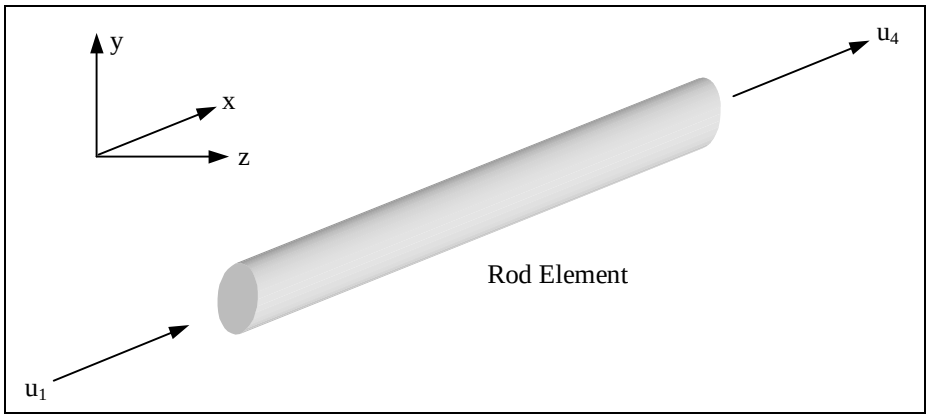

Figure 3. Rod Element

The elemental stiffness and mass matrices for the rod model, respectively, are shown in eqns 2.1 and 2.2.

$$k_{rod} = \begin{array}{c} \begin{matrix} u_1 & u_2 & u_3 & u_4 & u_5 & u_6 \end{matrix} \\ \begin{bmatrix} \frac{EA}{L} & 0 & 0 & \frac{-EA}{L} & 0 & 0 \\ 0 & 0 & 0 & 0 & 0 & 0 \\ 0 & 0 & 0 & 0 & 0 & 0 \\ \frac{-EA}{L} & 0 & 0 & \frac{EA}{L} & 0 & 0 \\ 0 & 0 & 0 & 0 & 0 & 0 \\ 0 & 0 & 0 & 0 & 0 & 0 \end{bmatrix} \end{array} \qquad (2.1)$$

$$m_{rod} = \frac{\rho AL}{12} \begin{bmatrix} 5 & 0 & 0 & 1 & 0 & 0 \\ 0 & 6 & 0 & 0 & 0 & 0 \\ 0 & 0 & 6 & 0 & 0 & 0 \\ 1 & 0 & 0 & 5 & 0 & 0 \\ 0 & 0 & 0 & 0 & 6 & 0 \\ 0 & 0 & 0 & 0 & 0 & 6 \end{bmatrix} \qquad (2.2)$$

In equation 2.1 and 2.2:

A = cross-sectional area

E = elastic modulus

L = length of element

ρ = density

2. Truss Construction

Table 1 shows the mass breakdown of the individual parts of the truss.

Quantity:	**Part name:**	**Individ. Mass:** (kg)
40	node balls	0.06625
100	longerons (unassembled)	0.01385
100	longerons (assembled)	0.04475
61	diagonals (unassembled)	0.02125
61	diagonals (assembled)	0.05215
322	bar end assemblies (each)	0.01545
322	screws (minus heat shrink & vibe tight)	0.60697 (total weight)
Assembled Truss	(bare, sum of above, assembled parts)	**11.7081**
Assembled Truss	(bare, actual measured mass)	**11.750**
Base plate	(not included in calculated or meas. mass)	7.30

Table 1. Truss Mass Breakdown

The Precision Space Truss was designed by and built at the Naval Research Lab. It was precisely assembled in the following manner. After each part was fabricated, the individual struts were assigned identifying serial numbers. These serial numbers were printed on tabs and attached to their respective members and covered with a transparent piece of heat shrink. In addition, each end assembly had the suffix of its strut's serial number etched on it in order that each two end assemblies remain permanently paired with their respective strut. End assemblies, without their struts, were first attached to their respective node balls. The node balls are aluminum spheres, approximately 38.7 mm in diameter (see Figure 2). Each node ball has eighteen connection points for attaching struts with end assemblies and for attaching thumb screws. A torque, socket wrench, set to 44 in-lbs., and fitted with a $9/64^{th}$ inch hex head was used to tighten the #8-32 screws which fasten the end assembly to the node ball. Each screw is prepared with heat shrink/vibe tight, which restricts a screw's ability to

loosen itself during prolonged, high frequency vibrations. After attaching the end assemblies to the node balls, the end assemblies were paired with their struts. An 11/16th torque wrench, set to 70 in-lbs. was used in conjunction with an open, ½ inch crescent wrench to tighten down the end assemblies on the struts.

B. DYNAMIC STIFFNESS TESTING

1. Introduction

In the case of the truss struts, I was interested in the effective axial stiffness from node-point to node-point (the center of a node ball is effectively a node-point). In other words, the effective axial stiffness of a strut was from the center of one node ball, to the next node ball, along the length of a truss element. The stiffness of individual parts was reasonably calculated. However, their combined, effective stiffness was not as easily obtained. A dynamic measurement procedure was devised by Robert Craig Waner at the Naval Research Lab for just such a measurement. For now, the effective axial stiffness of a rod element may be defined as follows:

$$k_{eff} = \left(\frac{AE}{L} \right)_{eff} \qquad (2.3)$$

where: A = cross-sectional area

E = Young’s modulus

L = length

2. Analytical Development

Struts can effectively be modeled as ~~a~~ springs with specific stiffness values (k_{eff}). The dynamic test for effective axial stiffness incorporated a system of two point masses (m_1 and m_2) connected by a linear spring (k_{eff}) as illustrated in Figure 4 (x_1 and x_2 are a global coordinate system).

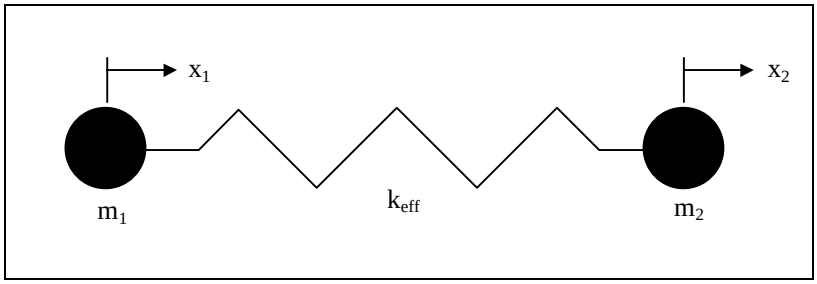

Figure 4. Schematic of Free-Free System

When we apply Newton's second law to the system we arrive at the following equations of motion:

$$m_1\ddot{x}_1 + k_{eff}x_1 - k_{eff}x_2 = 0 \qquad (2.4a)$$

$$m_2\ddot{x}_2 + k_{eff}x_2 - k_{eff}x_1 = 0 \qquad (2.4b)$$

Which results in the following matrix:

$$\begin{bmatrix} m_1 & 0 \\ 0 & m_2 \end{bmatrix}\begin{Bmatrix} \ddot{x}_1 \\ \ddot{x}_2 \end{Bmatrix} + \begin{bmatrix} k_{eff} & -k_{eff} \\ -k_{eff} & k_{eff} \end{bmatrix}\begin{Bmatrix} x_1 \\ x_2 \end{Bmatrix} = \begin{Bmatrix} 0 \\ 0 \end{Bmatrix} \qquad (2.5)$$

Assume a harmonic solution of the form in the following equation:

$\{x\} = \{x_0\} \cos(\omega t + \phi)$ (2.6)

where: $\{x_0\}$ = 2 by 1 vector of time-independent amplitudes

ω = undamped natural frequency of system

ϕ = phase angle

If we now substitute equation (2.6) and its derivatives into Equation (2.5), we will arrive at the new matrix below:

$$\begin{bmatrix} (-m_1\omega^2 + k_{eff}) & -k_{eff} \\ -k_{eff} & (-m_2\omega^2 + k_{eff}) \end{bmatrix} \begin{Bmatrix} x_{0_1} \\ x_{0_2} \end{Bmatrix} = \begin{Bmatrix} 0 \\ 0 \end{Bmatrix} \quad (2.7)$$

In this new matrix, equation (2.7), the vector $\{x_0\}$ is the nullspace of the left-hand matrix. Since every matrix has a null space, ω must be chosen such that the left-hand matrix has a nullspace. This dictates that the left-hand matrix must be singular, and therefore, its determinant must be equal to zero.

When we take the determinant of the left-hand matrix in equation (2.7), and set it equal to zero, we are left with the following expression:

$$m_1 m_2 \omega^4 - k_{eff} m_1 \omega^2 - k_{eff} m_2 \omega^2 = 0 \quad (2.8)$$

Solving equation (2.8) for ω^2:

$\omega^2 = 0$ (rigid body mode) (2.9a)

$$\omega^2 = \frac{k_{eff}(m_1 + m_2)}{m_1 m_2} \quad (2.9b)$$

Extracting k_{eff} from equation (2.9b) gives us the following expression for the effective stiffness:

$$k_{eff} = \frac{m_1 m_2 \omega^2}{(m_1 + m_2)} \quad (2.10)$$

3. Stiffness Experimental Implementation

To determine the effective axial stiffness of individual struts, an experiment was set up (see Figure 5), which included a strut (with terminating assemblies) and a single node ball bolted between two weights suspended by turnbuckles and two wires anchored at points ten feet above the floor. The outputs from both the accelerometer and the impulse hammer were fed into a Hewlett Packard, HP35670A, Dynamic Signal Analyzer (S/N 3431A01574). Finally, output from the HP Dynamic Signal Analyzer was saved to diskette and analyzed on a PC using MATLAB.

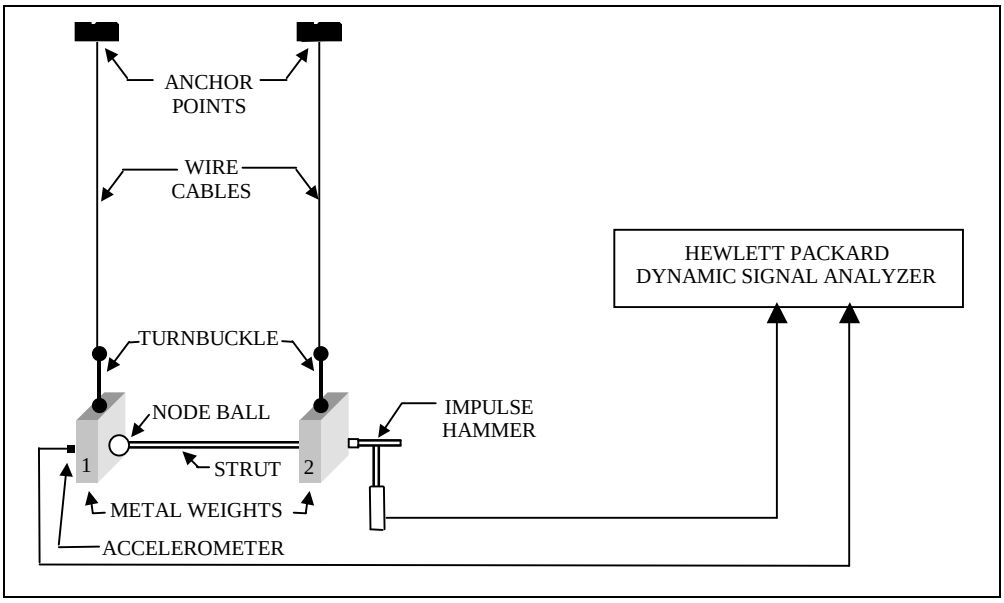

Figure 5. Effective Axial Stiffness Test Setup

The procedure consisted of tapping the metal block (weight) on the side opposite the accelerometer with the impulse hammer. The velocity vector of this tap should be parallel to the longitudinal axis of the strut. This impulse will excite the strut to its natural frequency. The accelerometer that was attached to the opposite metal block sensed the vibration. Using the Hewlett Packard Dynamic Signal Analyzer, a frequency response function (FRF) was generated. Referencing the largest peak in this FRF, a corresponding natural frequency can be determined. Recall that in our analytical development, equation (2.9a) predicted a rigid body mode ($\omega^2 = 0$). In the experimental model, we only approximated a free-free system (we had the wire cables to contend with, however negligible they were) whereas the analytical model is a true, free-free system. Once we know ω, the natural frequency, we need only know the total mass of the metal end blocks, m_1 and m_2, to

determine the effective stiffness, k_{eff}. m_1 consists of one metal block, the accelerometer, the node ball, one half of the tube mass, and an end assembly (outer sleeve, bolt, standoff, and nut; see Figure 2). m_2 consists of one metal block, one half of the tube mass, and an end assembly. We now have the values necessary to calculate the effective stiffness (see equation (2.10)).

4. Stiffness Experimental Results

Using the dynamic stiffness test, five different battens/longerons and five different diagonals were tested. Each element was tested five times to develop an average for that specific element. Then the five longeron averages and the five diagonal element averages were averaged to develop an effective axial stiffness for that type of element. In the following tables (Tables 2 and 3), effective stiffness determined by the dynamic test is $\mathbf{k_{eff}}$.

Battens/Longerons:				
Number	**f** (Hz)	(rad/sec)	$\mathbf{k_{eff}}$ (N/m)	$\mathbf{k_{eff}}$ (lb/in)
1	474.6	2982.000	7.44E+06	42499.79
2	470.9	2958.752	7.33E+06	41839.71
3	467.3	2936.132	7.22E+06	41202.43
4	473.9	2977.602	7.42E+06	42374.51
5	472.55	2969.119	7.38E+06	42133.43
		average =	7.36E+06	42009.98

Table 2. Batten/Longeron Effective Stiffness

Diagonal Elements:				
Number	**f** (Hz)	(rad/sec)	**k**eff (N/m)	**k**eff (lb/in)
1	391.5	2459.867	5.06E+06	28919.77
2	392	2463.009	5.08E+06	28993.69
3	374	2349.911	4.62E+06	26392.13
4	386.5	2428.451	4.94E+06	28185.80
5	388.5	2441.017	4.99E+06	28478.25
		average =	4.94E+06	28193.93

Table 3. Diagonal Effective Stiffness

C. BUILDING THE ANALYTICAL MODEL

We had already collected the truss properties required to build an accurate model of the structure. Specifically, we knew the masses of different elements, we knew the effective axial stiffness values for the longerons and diagonal elements, and we knew how the truss was constructed. Although these frequencies provided a good estimate to compare actual frequencies with, there were several limitations to the model.

The following table, Table 4, NPS Space Truss Natural Frequencies, corresponds to the first 20 natural frequencies, as computed by NRLFEMI. Table 5, NRL Truss Natural Frequencies, is also displayed for comparison. The original NRL truss had steel node balls in place of the Aluminum node balls present on the NPS Space Truss. The extra mass at the nodes forced the natural frequencies of the NRL truss lower then those of its NPS counterpart.

Number	ω_n(rad/s)	**frequency**(Hz)
1.00	92.01	14.64
2.00	102.14	16.26
3.00	191.06	30.41
4.00	213.44	33.97
5.00	395.40	62.93
6.00	468.36	74.54
7.00	506.79	80.66
8.00	634.66	101.01
9.00	793.12	126.23
10.00	854.35	135.97
11.00	885.68	140.96
12.00	1246.87	198.44
13.00	1305.21	207.73
14.00	1442.56	229.59
15.00	1461.82	232.66
16.00	1616.49	257.27
17.00	1762.29	280.48
18.00	1788.50	284.65
19.00	1970.66	313.64
20.00	2206.76	351.22

Table 4. NPS Precision Space Truss Natural Frequencies Using Aluminum Nodes (calculated)

Number	ω_n (rad/s)	**frequency**(Hz)
1.00	79.24	12.61
2.00	88.65	14.11
3.00	166.23	26.46
4.00	185.71	29.56
5.00	343.14	54.61
6.00	404.34	64.35
7.00	435.82	69.36
8.00	549.16	87.40
9.00	689.26	109.70
10.00	742.51	118.17
11.00	769.08	122.40
12.00	1079.98	171.88
13.00	1139.06	181.29
14.00	1246.46	198.38
15.00	1255.79	199.87
16.00	1404.31	223.50
17.00	1527.16	243.06
18.00	1548.73	246.49
19.00	1704.14	271.22
20.00	1902.63	302.81

Table 5. NRL Precision Space Truss Natural Frequencies Using Steel Nodes (calculated)

III. STRAIN-DISPLACEMENT MAPPING

This work assumes that only axial strain exists. The strain in an individual member can be calculated using

$$\varepsilon = \frac{(L_f - L_i)}{L_i} \qquad \textbf{(3.1)}$$

Where ε is the member strain and L_i and L_f are the original and final length of the member respectively. We assume the strain is due entirely to axial forces and bending does not occur in any elements of the structure. Figure 6 illustrates the displacement of a member under an arbitrary set of loads.

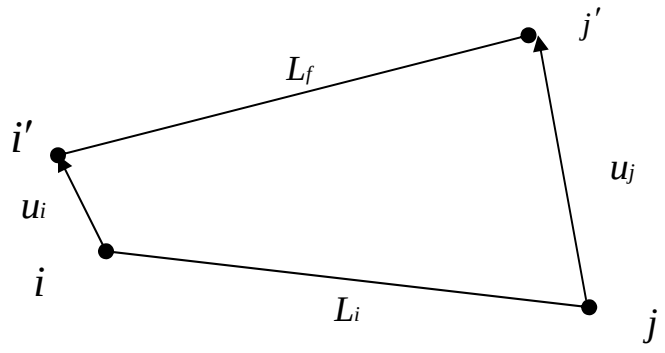

Figure 6. Displacement of an Arbitrary Member

Points i and j are displaced to i' and j' as shown by the respective displacement vectors u_i and u_j. The initial

length L_i is obtained from the coordinates corresponding to the undeformed endpoints.

$$L_i^2 = (x_i - x_j)^2 + (y_i - y_j)^2 + (z_i - z_j)^2 \qquad (3.2)$$

Consider the truss structure shown in Figure 7. If the coordinates of the nodes at n1, n2, n3, and n4 are given, the coordinates of the nodes at n5, n6, n7, and n8 can be computed from the strain measurements of the beam element.

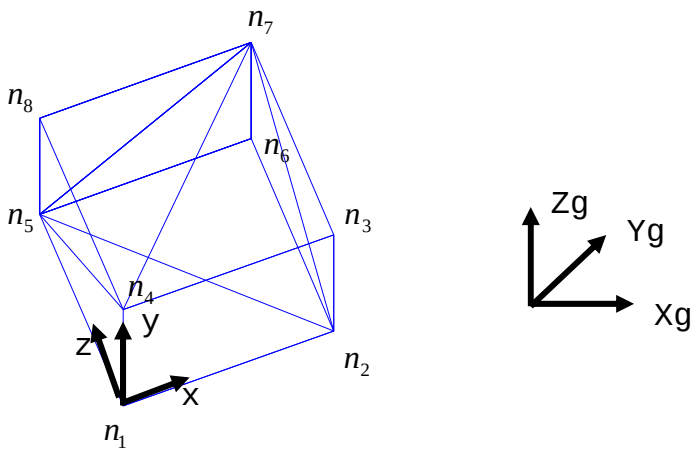

Figure 7. Local and Global Coordinates

First, local and global coordinates for the beam deformation are defined as shown in Figure 7. Local z-direction unit vector is identified as a direction perpendicular to the plane formed by n2-n1 and n4-n1 vectors such that

$$z = \frac{(n_2 - n_1) \times (n_4 - n_1)}{\left\| (n_2 - n_1) \times (n_4 - n_1) \right\|} \qquad (3.3)$$

Local x-direction is defined as

$$x = \frac{n_2 - n_1}{\left\| n_2 - n_1 \right\|} \qquad (3.4)$$

Then the local y-direction is defined as

$$y = z \times x \qquad (3.5)$$

The definition of the local axis uses small angle approximations cause by the deformation of the beam. However, this definition of the local coordinates will simplify the computation of displacement of the whole structure. The coordinates of the nodes n5, n6, n7, and n8 can be easily computed from the strain measurements of the beam elements in local coordinates, accounting only the axial deformation of each beam element. A transformation matrix transforms the coordinates of the computed nodes in local coordinates to the global coordinates. Since the local frame unit vectors are written as global coordinates in equations (3.3) through (3.5), the coordinate transformation matrix is simply written as

$$T = [x \quad y \quad z] \qquad (3.6)$$

To determine the deformation of the whole structure requires sequential computation of the succeeding nodes. Starting from the base of the structure with fixed coordinates (nodes 37, 38, 39, and 40), the coordinates of the next 4 nodes (nodes 3, 4, 12, and 13) are identified. Using the identified nodes as base nodes, the coordinates of the next 4 nodes can be computed. This procedure is repeated until the node coordinates for the whole structure are determined.

THIS PAGE INTENTIONALLY LEFT BLANK

IV. SIMULATION

The characteristics of the space truss were placed into the FEM program NASTRAN. This data was uploaded into PATRAN where a finite element analysis was performed on the structure. A static load was applied in the axial direction at Node 5 of the structure. The finite element analysis yielded the displacements at each node as well as the axial forces for each element.

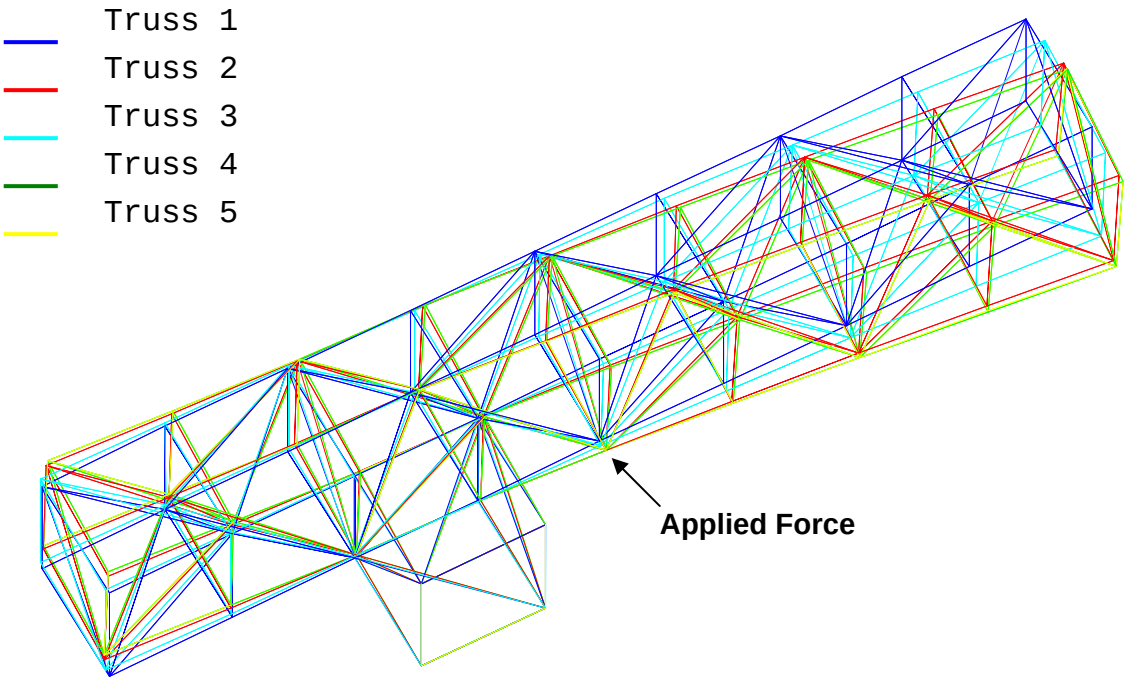

Figure 8. Truss Strain Analysis

In Figure 8, Truss 1 is the non-deformed truss before the force is introduced. Truss 2 is the result of the displacements calculated by NASTRAN. Truss 3 is the result of the strain calculated from the displacements but with none of the diagonals included. Truss 4 is the same as Truss 3 but with the diagonals of the two base bays, where most of the error originates, included. Truss 5 actually removes the strain values from two of the bays. The strains in these areas are interpolated, since the strain is assumed to be linear from the base to the end.

The objective of this thesis was to see if the strain measurements alone could approximate the end point deflection observed using the displacement values from NASTRAN. Table 6 shows a quantitative assessment of the strain based measurements and the NASTRAN results.

NASTRAN	Truss 3	Truss 4	Truss 5
# of strain measurements	56	64	48
Deformation(mm) at 36 x = 0.0234E-4 y = -0.1086E-4 z = 0.0685E-4	x = 0.0866E-5 y = -0.5942E-5 z = 0.2647E-5	x = 0.0259E-4 y = -0.1177E-4 z = 0.0839E-4	x = 0.0255E-4 y = -0.1176E-4 z = 0.0839E-4
Deformation(mm) at 19 x = 0.0439E-4 y = -0.1089E-4 z = 0.0685E-4	x = 0.2182E-5 y = -0.5918E-5 z = 0.2647E-5	x = 0.0502E-4 y = -0.1174E-4 z = 0.0839E-4	x = 0.0499E-4 y = -0.1174E-4 z = 0.0839E-4
Deformation(mm) at 9 x = -0.0005E-4 y = -0.1086E-4 z = 0.0676E-4	x = -0.0619E-5 y = -0.5726E-5 z = 0.2854E-5	x = 0.0005E-4 y = -0.1155E-4 z = 0.0837E-4	x = 0.0002E-4 y = -0.1154E-4 z = 0.0837E-4
Deformation(mm) at 18 x = 0.0164E-4 y = -0.1089E-4 z = 0.0676E-4	x = 0.0335E-5 y = -0.5918E-5 z = 0.2854E-5	x = 0.0201E-4 y = -0.1174E-4 z = 0.0837E-4	x = 0.0196E-4 y = -0.1174E-4 z = 0.0837E-4
% error at node 36	49.7%	12.5%	12.4%
% error at node 19	49.7%	12.4%	12.3%
% error at node 9	49.8%	11.5%	11.5%
% error at node 18	49.1%	12.6%	12.5%

Table 6. Deformation of the truss at the end nodes

The x, y and z displacements at the end of the structure computed from a Nastran simulation are shown in the first column. The displacements computed from the strain measurements appear in columns 2, 3 and 4. As mentioned above, Truss 3 does not include the strains in the diagonals. Truss 4 includes the diagonals for the two base bays, and Truss 5 interpolates the strains for the bay to right of the Nodes 5 and 7. The error was computed from the total RMS deviation of the x, y and z components of the Nastran and strain calculations. Although none of the strain based displacements were very accurate, there were some observations that were expected. It is clear that the more strain measurements available the more accurate the mapping. Something that was not expected was the similarity between trusses 4 and 5. This result shows that, at some point, there is not much difference between having the strain measurements and using interpolated values.

THIS PAGE INTENTIONALLY LEFT BLANK

V. CONCLUSIONS AND RECOMMENDATIONS

This work has shown that strain can be used to measure displacement of a space truss to an accuracy of 12%. From these measurements, bending modes can be predicted, although not very accurately unless many strain gauges are used. Additionally, this work has shown that on this type of a truss, the base bays should have a greater density of strain gauges than other locations. Future work should include the employment of many more strain gauges to see if a modeshape can in fact be predicted. In addition, the assumption that only axial strain exists with no bending should be abandoned, even though this makes the problem much more difficult. Another assumption that I made was that the displacement was distributed equally on either side of each element. I know now that this was probably a large source of error since the diagonal element would tend to bend one side more than the other.

Future work without the aforementioned assumptions could result in a procedure for the real-time determination of displacements at any point of a vibrating body using strain gauges. The procedure could employ measurement devices like Fiber Bragg Gratings, which are capable of very fine strain measurements. This thesis presents the finite element analysis of a truss similar to the NPS Space truss to observe the behavior of the strain relative to the displacement.

THIS PAGE INTNETIONALLY LEFT BLANK

APPENDIX

The following MATLAB functions use the strain values from NASTRAN to compute displacements in local coordinates of the deformed truss. Another function builds a transformation matrix needed to convert the local coordinates to global coordinates. Next the coordinates are used to draw the deformed truss.

```
function n_prime = ndisp(n,st)

% function ndisp calculates coordinates of deformed nodes due to the
strain
% n: coordinate of the starting nodes
% n = [n1x n1y n1z
%     n2x n2y n2z
%     n3x n3y n3z
%     n4x n4y n4z]
% st: length and strain of each bar element
% st = [L1 s1
%       L2 s2
%       L3 s3
%       L4 s4
%       L5 s5
%       L6 s6
%       L7 s7
%       L8 s8]

% compute displacement change due to the bar length and strain in local
coordinates
deltad = [-0.5*st(5,1)*st(5,2) -0.5*st(8,1)*st(8,2)
st(1,1)+st(1,1)*st(1,2);...
    0.5*st(5,1)*st(5,2) -0.5*st(6,1)*st(6,2)
st(2,1)+st(2,1)*st(2,2);...
    0.5*st(7,1)*st(7,2) 0.5*st(6,1)*st(6,2) st(3,1)+st(3,1)*st(3,2);...
    -0.5*st(7,1)*st(7,2) 0.5*st(8,1)*st(8,2) st(4,1)+st(4,1)*st(4,2)];

% compute the transformation matrix from local coordinates to global
% coordinates
```

```
e1 = (n(2,:)-n(1,:))'/norm(n(2,:)-n(1,:));
e2p = (n(4,:)-n(1,:))'/norm(n(4,:)-n(1,:));
e3p = cross(e1,e2p);
e3 = e3p/norm(e3p);
e2 = cross(e3,e1);
T = [e1 e2 e3];


% displacement change in global coordinates
d1 = T*deltad(1,:)';
d2 = T*deltad(2,:)';
d3 = T*deltad(3,:)';
d4 = T*deltad(4,:)';

% global coordinates of the deformed end nodes
n_prime = n+[d1';d2';d3';d4'];
function n_prime = ndispdiag(n,st)

% function ndisp calculates coordinates of deformed nodes due to the
strain
% n: coordinate of the starting nodes
% n = [n1x n1y n1z
%     n2x n2y n2z
%     n3x n3y n3z
%     n4x n4y n4z]
% st: length and strain of each bar element
% st = [L1 s1
%       L2 s2
%       L3 s3
%       L4 s4
%       L5 s5
%       L6 s6
%       L7 s7
%       L8 s8
%       L9 s9
%       L10 s10
%       L11 s11
%       L12 s12]


% compute displacement change due to the bar length and strain in local
coordinates
L1 = st(1,1);L2 = st(2,1);L3 = st(3,1);L4 = st(4,1);L5 = st(5,1);L6 =
st(6,1);
```

```
L7 = st(7,1);L8 = st(8,1);L9 = st(9,1);L10 = st(10,1);L11 =
st(11,1);L12 = st(12,1);

s1 = st(1,2);s2 = st(2,2);s3 = st(3,2);s4 = st(4,2);s5 = st(5,2);s6 =
st(6,2);
s7 = st(7,2);s8 = st(8,2);s9 = st(9,2);s10 = st(10,2);s11 =
st(11,2);s12 = st(12,2);

n1 = n(1,:);
n2 = n(2,:);
n3 = n(3,:);
n4 = n(4,:);

d1 = L1*s1;
d2 = L2*s2;
d3 = L3*s3;
d4 = L4*s4;
d5 = L5*s5;
d6 = L6*s6;
d7 = L7*s7;
d8 = L8*s8;
d9 = L9*s9;
d10 = L10*s10;
d11 = L11*s11;
d12 = L12*s12;

a1a = acos(((L1+d1)^2+norm(n2-n1)-(L2+d2)^2)/(2*(L1+d1)*norm(n2-n1)));
a3a = acos(((L5+d5)^2+norm(n3-n2)-(L4+d4)^2)/(2*(L5+d5)*norm(n3-n2)));
a1b = acos(((L1+d1)^2+norm(n4-n1)-(L8+d8)^2)/(2*(L1+d1)*norm(n4-n1)));
a3b = acos(((L5+d5)^2+norm(n4-n3)-(L6+d6)^2)/(2*(L5+d5)*norm(n4-n3)));

deltad = [-(L1+d1)*cos(pi-a1a) -(L1+d1)*cos(pi-a1b)
(L1+d1)*sin(pi-a1a);...
    d9-(L1+d1)*cos(pi-a1a) -d10+(L5+d5)*cos(pi-a3a) L3+d3;...
    (L5+d5)*cos(pi-a3b) (L5+d5)*cos(pi-a3a) (L5+d5)*sin(pi-a3a);...
    -d11+(L5+d5)*cos(pi-a3b) d12-(L1+d1)*cos(pi-a1b) L7+d7];



% compute the transformation matrix from local coordinates to global
% coordinates
e1 = (n(2,:)-n(1,:))'/norm(n(2,:)-n(1,:));
e2p = (n(4,:)-n(1,:))'/norm(n(4,:)-n(1,:));
e3p = cross(e1,e2p);
```

```
e3 = e3p/norm(e3p);
e2 = cross(e3,e1);
T = [e1 e2 e3];

% displacement change in global coordinates
d1 = T*deltad(1,:)';
d2 = T*deltad(2,:)';
d3 = T*deltad(3,:)';
d4 = T*deltad(4,:)';

% global coordinates of the deformed end nodes
n_prime = n+[d1';d2';d3';d4'];


% truss coordinates
n(1,:) = [0 0 0];
n(2,:) = [1 0 0];
n(3,:) = [2 0 0];
n(4,:) = [3 0 0];
n(5,:) = [4 0 0];
n(6,:) = [5 0 0];
n(7,:) = [6 0 0];
n(8,:) = [7 0 0];
n(9,:) = [8 0 0];

n(10,:) = [0 0 -1];
n(11,:) = [1 0 -1];
n(12,:) = [2 0 -1];
n(13,:) = [3 0 -1];
n(14,:) = [4 0 -1];
n(15,:) = [5 0 -1];
n(16,:) = [6 0 -1];
n(17,:) = [7 0 -1];
n(18,:) = [8 0 -1];

n(19,:) = [8 1 -1];
n(20,:) = [7 1 -1];
n(21,:) = [6 1 -1];
n(22,:) = [5 1 -1];
n(23,:) = [4 1 -1];
n(24,:) = [3 1 -1];
n(25,:) = [2 1 -1];
n(26,:) = [1 1 -1];
n(27,:) = [0 1 -1];
```

```
n(28,:) = [0 1 0];
n(29,:) = [1 1 0];
n(30,:) = [2 1 0];
n(31,:) = [3 1 0];
n(32,:) = [4 1 0];
n(33,:) = [5 1 0];
n(34,:) = [6 1 0];
n(35,:) = [7 1 0];
n(36,:) = [8 1 0];

n(37,:) = [2 -1 -1];
n(38,:) = [3 -1 -1];
n(39,:) = [2 -1 0];
n(40,:) = [3 -1 0];
```

% displacements

```
d(1,:) = [ 0.0000006433343   0.0000031524010    -0.0000020019660 ];
d(2,:) = [ 0.0000006432649   0.0000017776800    -0.0000013283960 ];
d(3,:) = [ 0.0000006431954   0.0000003913266    -0.0000006431954 ];
d(4,:) = [ 0.0000004920491   -0.0000002155565   -0.0000001560156 ];
d(5,:) = [ 0.0000003409029   -0.0000021745580   0.0000008862774 ];
d(6,:) = [ 0.0000002266914   -0.0000039949240   0.0000020054920 ];
d(7,:) = [ 0.0000001124798   -0.0000061284770   0.0000034378920 ];
d(8,:) = [ 0.0000000305816   -0.0000083475000   0.0000049557630 ];
d(9,:) = [ -0.0000000513165  -0.0000108571000   0.0000067642150 ];
d(10,:) = [ 0.0000013170040  0.0000030943180    -0.0000020019660 ];
d(11,:) = [ 0.0000013170040  0.0000017253920    -0.0000013283960 ];
d(12,:) = [ 0.0000013091220  0.0000001840490    -0.0000006431954 ];
d(13,:) = [ 0.0000013012410  -0.0000004078845   -0.0000001560156 ];
d(14,:) = [ 0.0000013951940  -0.0000022072980   0.0000008862774 ];
d(15,:) = [ 0.0000014891470  -0.0000039297900   0.0000020054920 ];
d(16,:) = [ 0.0000015644640  -0.0000061383070   0.0000034378920 ];
d(17,:) = [ 0.0000016397810  -0.0000082613540   0.0000049557630 ];
d(18,:) = [ 0.0000016397810  -0.0000108930300   0.0000067642150 ];
d(19,:) = [ 0.0000043888120  -0.0000108930300   0.0000068456460 ];
d(20,:) = [ 0.0000040711050  -0.0000082613540   0.0000049151220 ];
d(21,:) = [ 0.0000037533970  -0.0000061383070   0.0000034932270 ];
d(22,:) = [ 0.0000034680030  -0.0000039297900   0.0000019858620 ];
d(23,:) = [ 0.0000031826090  -0.0000022072980   0.0000009645222 ];
d(24,:) = [ 0.0000029341500  -0.0000004078845   -0.0000001337391 ];
```

```
d(25,:) = [ 0.0000026856910  0.0000003680981    -0.0000007360339 ];
d(26,:) = [ 0.0000026857600  0.0000017253920    -0.0000013921760 ];
d(27,:) = [ 0.0000026858300  0.0000030943180    -0.0000020599500 ];
d(28,:) = [ 0.0000020181560  0.0000031524010    -0.0000020599500 ];
d(29,:) = [ 0.0000020181560  0.0000017776800    -0.0000013921760 ];
d(30,:) = [ 0.0000020102740  0.0000003913266    -0.0000007360339 ];
d(31,:) = [ 0.0000020023930  -0.0000004311130   -0.0000001337391 ];
d(32,:) = [ 0.0000020963460  -0.0000021745580   0.0000009645222 ];
d(33,:) = [ 0.0000021902990  -0.0000039949240   0.0000019858620 ];
d(34,:) = [ 0.0000022656160  -0.0000061284770   0.0000034932270 ];
d(35,:) = [ 0.0000023409330  -0.0000083475000   0.0000049151220 ];
d(36,:) = [ 0.0000023409330  -0.0000108571000   0.0000068456460 ];
d(37,:) = [ 0.0000000000000  0.0000000000000    0.0000000000000 ];
d(38,:) = [ 0.0000000000000  0.0000000000000    0.0000000000000 ];
d(39,:) = [ 0.0000000000000  0.0000000000000    0.0000000000000 ];
d(40,:) = [ 0.0000000000000  0.0000000000000    0.0000000000000 ];

nd = n+30000*d;
drawtruss(n,'b')
drawtruss(nd,'r')

function drawtruss(n,clr)

%n: 40x3 node coordinates data set

%connectivity

c{1} = [2 10 11 27 28 29];
c{2} = [1 3 11 29];
c{3} = [2 4 11 12 13 29 30 31];
c{4} = [3 5 13 31];
c{5} = [4 6 13 14 15 31 32 33];
c{6} = [5 7 15 33];
c{7} = [6 8 15 16 17 33 34 35];
c{8} = [7 9 17 35];
c{9} = [8 17 18 19 35 36];
c{10} = [1 11 27];
c{11} = [1 2 3 10 12 25 26 27 29];
c{12} = [3 11 13 25];
c{13} = [3 4 5 12 14 23 24 25 31];
c{14} = [5 13 15 23];
c{15} = [5 6 7 14 16 21 22 23 33];
c{16} = [7 15 17 21];
c{17} = [7 8 9 16 18 19 20 21 35];
```

```
c{18} = [9 17 19];
c{19} = [9 18 20 35 36];
c{20} = [17 19 21 35];
c{21} = [7 15 16 17 20 22 33 34 35];
c{22} = [15 21 23 33];
c{23} = [5 13 14 15 22 24 31 32 33];
c{24} = [13 23 25 31];
c{25} = [3 11 12 13 24 26 29 30 31];
c{26} = [11 25 27 29];
c{27} = [1 10 11 26 28 29];
c{28} = [1 27 29];
c{29} = [1 2 3 11 25 26 27 28 30];
c{30} = [3 25 29 31];
c{31} = [3 4 5 13 23 24 25 30 32];
c{32} = [5 23 31 33];
c{33} = [5 6 7 15 21 22 23 32 34];
c{34} = [7 21 33 35];
c{35} = [7 8 9 17 19 20 21 34 36];
c{36} = [9 19 35];
c{37} = [3 12 13 38];
c{38} = [13 37 40];
c{39} = [3 37 40];
c{40} = [3 4 13 38 39];

for i = 1:40,
    for j = 1:length(c{i})
        drawline(n(i,:),n(c{i}(j),:),clr)
    end
end
```

THIS PAGE INTENTIONALLY LEFT BLANK

LIST OF REFERENCES

1. Gaukroger, D.R. and Hassal, C.J., “Measurement of Vibratory Displacements of a Rotating Blade”, Vertica, Vol.2, pp. 111-120, 1978.
2. Foss, G.C. and Haugse, E.D., “Using Modal Test Results to Develop Strain to Displacement Transformations”, Proceedings of the 13th International Modal Analysis Conference, pp. 112-118, February 1995.
3. Davis, M.A., Kersey, A.D., Sirkis, J. and Frieble, E.J., “Fiber Optic Bragg Grating Array for Shape and Vibration Mode Shape Sensing”, SPIE Vol. 2191, Paper #10, Orlando, FL, 1994.
4. Kirby, G.C., Lindner, D.K., Davis, M.A. and Kersey, A.D., “Optimal Sensor Layout for Shape Estimation From Strain Sensors”, SPIE Vol. 2444 pp.367-376, 1995.
5. Baz, A., Poh, S., Ro, J., “Cross-Over Monitoring of a Transverse Bridge”, Belvoir R D &E Center, Combat Engineering Directorate, Bridge Division, Fort Belvoir, VA, Contract # DAAK70-93-V-0270.
6. Gopinathan, M., Pajunen, G. A., Nellakanta, P.S., and Arockasissamy, M., “Recursive Estimation of Displacement and Velocity in a Cantilever Beam Using a Measured Set of Distributed Strain Data”, J. Intel. Mat. Sys. And Struct, Vol. 6, No. 4 pp. 537-549, 1995.
7. Vurpillot, S., Inaudi, D., Scano, A., “Mathematical Model for the Determination of Vertical Displacement

From Internal Horizontal Measurements of a Bridge", SPIE Vol 2719, Paper # 5, San Diego, CA, 1996.

8. Anderson, M.S. and Crawley, E.F., "Structural Shape Estimation Using Shaped Sensors", Proceedings of the 36th AIAA/ASME/ASCE/AHS/ASC Structures, Structural Dynamics and Materials Conference, Vol. 5, pp. 3368-3378, April 1995.
9. Pantling, Carey M., *Active Vibration Control Method for Space Truss Using Piezoelectric Actuators and Finite Elements*, Master's Thesis, Naval Postgraduate School, Monterey, CA, December 1999.
10. Meirovitch, L. and Baruh, H., "The Implementation of Modal Filters for Control of Structures", Journal of Guidance, Vol. 8, No. 6 pp. 707-715, 1985.
11. Johnson, Scott E. and Vlattas, John, *Modal Analysis and Active Vibration Control of the Naval Postgraduate School Space Truss*, Master's Thesis, Naval Postgraduate School, Monterey, CA, June 1998.
12. Andberg, Brent K., *Modal Testing and Analysis of the NPS Space Truss*, Master's Thesis, Naval Postgraduate School, Monterey, CA, September 1997.

INITIAL DISTRIBUTION LIST

1. Defense Technical Information Center
   8725 John J. Kingman Rd., STE 0944
   Ft. Belvoir, VA 22060-6218

2. Dudley Knox Library
   Naval Postgraduate School
   Monterey, CA 93943-5000